ELSEVIER

Journal of Electron Spectroscopy and Related Phenomena 117–118 (2001) 383–395

JOURNAL OF ELECTRON SPECTROSCOPY and Related Phenomena

www.elsevier.nl/locate/elspec

Resonant inverse photoemission study on strongly correlated systems

K. Kanai[a], S. Shin[a,b,*]

[a]*The Institute of Physical and Chemical Reearch (RIKEN), Sayo-gun, Hyogo 679-5148, Japan*
[b]*Institute for Solid State Physics, University of Tokyo, 5-1-5 Kashiwanoha, Kashiwa, Chiba 277-8581, Japan*

Abstract

We have performed resonant inverse photoemission (RIPE) spectroscopy on the transition metal and rare-earth metal compounds in the ultraviolet energy region. We present, here, some characteristics of the RIPE spectra of several intermetallic Ce compounds at the Ce-$N_{4,5}$ absorption edge. Clear RIPE spectra are observed. From the comparison between the experimental and the calculated spectra, the resonance behaviors can be well explained within the localized picture of the 4f electrons. On the other hand, the information about the fractional 4f occupancy in the systems with high Kondo temperature is strongly reflected in the intensities of the coherent and incoherent components of RIPE spectra. The RIPE spectra sensitively detect the variations in the 4f electronic states by destruction of the collective Kondo state, with increasing temperature. We can derive direct information about the temperature and T_K dependence of the 4f electronic states from the spectra. On the other hand, it is necessary to take the surface contributions into account in order to derive quantitative information. We present an example of the analysis of RIPE spectra at $N_{4,5}$ pre-threshold, including both contributions from the bulk and surface.

Keywords: RIPE spectroscopy; Intermetallic Ce compounds; Surface effect on RIPE spectra; Kondo-scaling

1. Introduction

Many transition metal and rare earth metal compounds are particularly attractive because they provide opportunities to challenge fundamental problems in solid state physics such as electron correlation. It is of great importance to investigate the electronic structure around the Fermi level E_F of these strongly correlated electronic (SCE) systems in order to understand their fascinating low temperature physical properties. Photoemission (PE) and inverse photoemission (IPE) spectroscopy are suitable techniques to serve this purpose. The combination of PE and IPE spectra give the most direct information about the density of state (DOS) around E_F. It is especially helpful to probe the unoccupied DOS of the SCE systems to investigate the excited states of the system which govern the transport and magnetic properties. The IPE spectrum gives a replica of the unoccupied DOS in the first approximation. However it is known that the IPE signal level is inherently low due to its extremely small cross section. Supposing that the IPE process is normally considered as the time-reversed version of the PE process, the PE cross section is $\sim 10^5$ times larger than that of the IPE, typically in ultraviolet (UV) energy region, and this is the reason that IPE spectroscopy is a more difficult experiment. Such difference in the cross section

*Corresponding author. Tel.: +81-471-363-381; fax: +81-471-363-383.
E-mail address: shin@issp.u-tokyo.ac.jp (S. Shin).

0368-2048/01/$ – see front matter
PII: S0368-2048(01)00259-6

between the PE and the IPE reflects the difference in the phase space available for photon or electron creation. One way to overcome the weakness of the IPE signal is application of the resonance effect to the IPE spectroscopy, which is a famous technique for PE spectroscopy. The resonance effect, which is related to the Fano effect in PE, brings about dramatic enhancement of the IPE cross section, and this technique is called 'resonant IPE (RIPE) spectroscopy'. The first observation of RIPE spectra was done on the La M_5 absorption edge by Liefield et al. in 1974 [1,2]. And, several years ago, Baer et al. applied RIPE spectroscopy to the investigation of the SCE systems [3–7]. They performed RIPE measurements on the Ce M_5 edge of several 'Ce-based Kondo materials'. Their results demonstrated the dramatic enhancements of the Ce 4f-IPE spectra when the excitation energy E_{ex} is tuned to the Ce 3d-binding energy. Tanaka and Jo first applied calculation within the impurity Anderson model (IAM) to the RIPE spectra [8,9]. Their calculation explains well the resonance behaviors of observed RIPE spectra at the Ce M_5 edge, which includes the full multiplet coupling effects and configuration dependent hybridization strength between the 4f and conduction electrons. On the other hand, the comparison between the experimental and calculated results of the RIPE spectra at the Ce $N_{4,5}$ edge of several Ce compounds are reported by Kanai et al. [10]. Clear resonant spectra were observed at the $N_{4,5}$ edge because of well separated incoherent components, i.e. the normal fluorescence from the RIPE spectra. This is reminiscent of the RPE (resonant photoemission) spectra at the $N_{4,5}$ edge [11]. Ishii et al., on the other hand, reported the RIPE study on NiS_2 at the Ni $M_{2,3}$ edge [12]. RIPE spectroscopy has developed into the most powerful tool to probe the unoccupied electronic structure of the SCE systems. The aim of this paper is to explain some of the characteristics of the RIPE spectra in the UV energy range. We take, here, the Ce $N_{4,5}$-RIPE spectra of several intermetallic Ce compounds as examples.

2. Resonant inverse photoemission spectroscopy

Fig. 1 shows a schematic process of RIPE of the Ce compounds. For simplicity the multiplet splitting of the 4f level is left out of consideration. If the excitation energy E_{ex} is tuned to the 4d binding energy, the RIPE process which is a second order optical process takes place. The generic process involved in RIPE can be thought of as having two steps: (1) after the electron entered into the empty state above the vacuum level, the electron falls into the 4f level (α). Simultaneously the 4d core electron jumps into another 4f level (β) by excess energy. This process is a reverse of the super Coster–Kronig process and occurs via Coulomb interaction. This radiationless process arrives at the intermediate state $|\underline{4d}, 4f^{n+2}, \underline{c}^n\rangle$, where $\underline{4d}$ and $\underline{c}$ represent the holes of the 4d-core and in the conduction band, respectively. This intermediate state is typically modeled as discrete, while the initial state $|4f^n, \underline{c}^n\rangle + E_{ex}$ has a continuum character associated with the range of

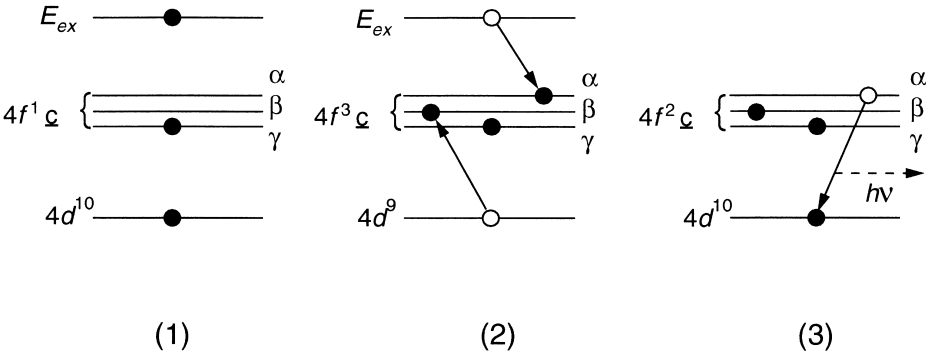

Fig. 1. Schematic RIPE process. (1), (2) and (3) represent the initial, intermediate and final states, respectively. For explanation, a $4f^1\underline{c}$ initial state is shown.

E_{ex}. (2) The 4f electron recombines the 4d-core hole and a photon $h\nu$ is emitted by the electric dipole transition. The processes (1) and (2) take place coherently. The initial $|4f^n, \underline{c}^n\rangle$ and final state $|4f^{n+1}, \underline{c}^n\rangle$ are the same as those of the normal IPE process and it is impossible to tell whether the process follows a normal or resonant path. Therefore the processes quantum mechanically interfere with each other. The probability for that resonant transition is described within the simple formalism by Fano and the total yield (TY) curve has the well-known Fano-type lineshape [13]. The 4f cross section σ_{4f} resonantly increases above the threshold. On the other hand the interference of the paths is known to decrease the cross section just below the threshold and to create a dip in the total yield (TY). Consequently, the TY has an asymmetric lineshape. For example, the decrease of the $3d^{10}$ component in RIPE spectra of the Ni as increasing the E_{ex} around the Ni-$M_{2,3}$ threshold is actually found by Tezuka et al. [14,15] and its theoretical support was given by Tanaka et al. [16]. And this so-called 'anti-resonance' behavior gives a direct confirmation about the existence of $3d^8$ initial state configuration in Ni, consistently with the RPE results [17]. In fact the $3d^9$ configuration does not contribute to the RIPE spectra because a single 3d hole does not allow the excitation process (1).

Finally, we make mention of the multiplet splitting in a more realistic case of a RIPE spectrum. The intermediate state of the RIPE process of Ce compounds actually splits off due to the 4d-core hole spin–orbit interaction and strong 4d–4f exchange interaction. It is indispensable to take those splittings into account, for the interpretation of RIPE spectra of Ce compounds, especially the E_{ex} dependence.

3. Experiment

Our experimental system is illustrated in Fig. 2. Measurements are performed in an ultrahigh vacuum (UHV) chamber where the pressure is about 5×10^{-11} Torr under the operation of an electron-gun.

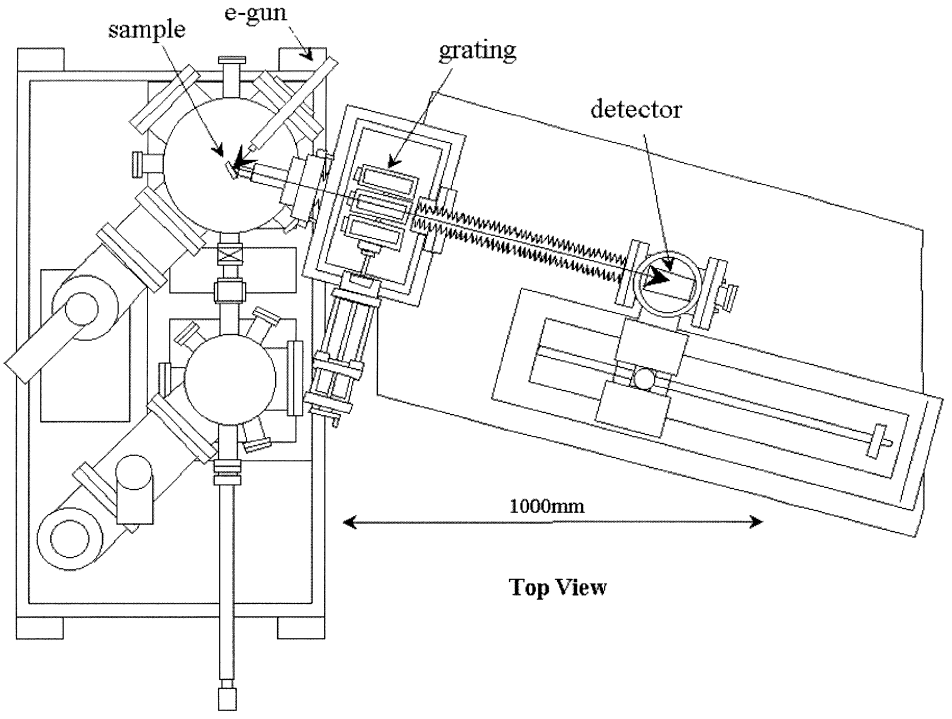

Fig. 2. The illustration of the experimental system for RIPE spectroscopy.

We use a thermal-cathode (BaO) electron-gun as an excitation source. Sample temperature is kept by the combination of a closed cycle ^{4}He refrigerator and a heater. Clean sample surfaces of a polycrystalline samples are obtained by scraping the surface with a diamond file in a UHV every 40–60 min at measurement temperature. The IPE spectra are measured by the soft X-ray emission system which has a Rowland mounted-type spectrometer [18]. This spectrometer is composed of three spherical gratings ($R=4$, 5, 10 m) and available in a wide energy range between 30 and 1200 eV. By this system, we can perform RIPE measurements at the transition metal $L_{2,3}$, $M_{2,3}$ edge and $M_{4,5}$, $N_{4,5}$ edge of most rare-earths. The signals are detected by a micro-channel plate and a one-dimensional position sensitive detector. The E_F position is determined by referring to the Fermi-edge in the IPE spectra of Au which is evaporated on the sample holder. The estimated total energy resolution at 100 eV is about 0.5 eV.

4. Resonant inverse photoemission spectra of Ce compounds

It is known that the X-ray absorption spectrum (XAS) at the $N_{4,5}$ edge of the mixed-valent Ce compound is composed of the following two parts; (1) a 'giant-absorption' band corresponding to dipole-allowed transition above the $N_{4,5}$-threshold; (2) a weak absorption region corresponding to dipole-forbidden transitions at the 'pre-threshold' [19]. In this paper, the RIPE spectra which are measured above and below the edge are called 'giant-resonance' and 'pre-threshold-resonance', respectively, after the XAS case.

4.1. Resonance effects of the giant-resonance

The off resonant-RIPE spectra of $CeRh_3$, $CePd_3$ and $CeSn_3$ are shown in Fig. 3a. The spectra are measured around $E_{ex}=90$ eV to obtain larger 4f contribution. Considerably different lineshapes of the off resonant spectra indicate the difference of their unoccupied states. The strong peak at 1.1 eV above E_F in the spectrum of $CeRh_3$ is the 'f^1 peak', which corresponds to the $4f^1$ final state. The f^1 peak contains the Kondo resonance, but its side-band

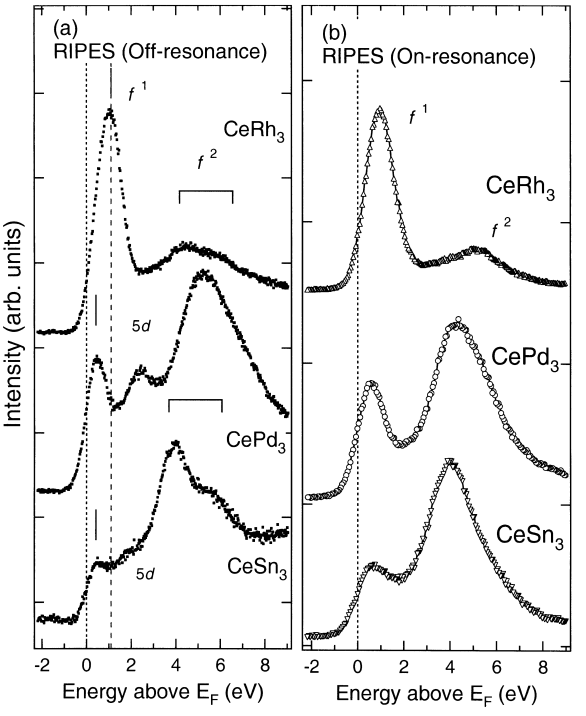

Fig. 3. (a) The off resonant RIPE spectra of $CeRh_3$, $CePd_3$ and $CeSn_3$. The abscissa is the energy above Fermi level (E_F). The measurements were performed at 25 K. (b) The on-resonant RIPE spectra of $CeRh_3$, $CePd_3$ and $CeSn_3$.

caused from the spin–orbit and crystal field excitations of $4f^1$ final state are convoluted with the experimental energy resolution. Thus the present f^1 peak position in the experiment does not exactly show Kondo temperature, k_BT_K, though the peak energy of 1.1 eV is much larger than the experimental resolution in $CeRh_3$.

The f^1 peaks of $CePd_3$ and $CeSn_3$ in Fig. 3a are at 0.5 eV. The T_Ks of $CePd_3$ and $CeSn_3$ are around 200 K so that the energy positions of f^1 peaks are mainly determined by the energy resolution [20,21]. The f^1 peak of $CeRh_3$ is much larger and it is situated at the higher energy side as compared with those of $CePd_3$ and $CeSn_3$. This indicates the extremely higher T_K and strong itinerant character of the 4f electron of $CeRh_3$ than that of the typical valence-fluctuating systems [22].

The structures corresponding to the final state with $4f^2\underline{c}$ configuration are observed around 5 eV in the spectra of $CeRh_3$ and $CePd_3$ and 4 eV in $CeSn_3$.

These broad bands are called the 'f^2 peak'. The f^2 peaks are found to have strong multiplet splitting which causes complicated lineshapes, as clearly shown in $CeRh_3$ and $CeSn_3$ spectra. On the other hand, the structures at 2 eV in the spectra of $CePd_3$ and $CeSn_3$ are assigned to the Ce 5d band. It seems to be difficult to estimate the parameters of the f peaks, for example for the energy positions and intensities, without subtracting the non-f background (mainly, Ce 5d band and ligand 4d band). This problem can be solved using the following resonant measurement.

Fig. 3b shows the on-resonant RIPE spectra of $CeRh_3$, $CePd_3$ and $CeSn_3$. The E_{ex} are chosen in order to drastically enhance the f^1 peak for each system. The Ce 5d band is not found in the spectra of $CePd_3$ and $CeSn_3$ due to the resonance-enhancement of 4f components. Reduction of spectral intensity at E_F in the on-resonant spectrum of $CeRh_3$ is caused by the lack of the 5d band contribution just above E_F. Thus, the on-resonance spectra in Fig. 3b can be regarded as the 4f contribution itself.

The f^1 peak intensity of $CeRh_3$ is extremely large as compared with those of $CePd_3$ and $CeSn_3$. Furthermore, the intensity at E_F is small. This directly reflects the highest T_K and that the $4f^0$ configuration is dominant in the initial state. This is consistent with the extremely low value of Pauli-like susceptibility χ_0 of $CeRh_3$ [23,24]. The remarkable itinerant character of 4f electron of $CeRh_3$ is reflected by the strongly depressed f^2 peak. The $CeRh_3$ can be regarded as the most α-like Ce compound. Similar remarkable properties are reported for $CePd_7$ [25].

The f^1 peak of $CeSn_3$, which is not seen clearly in the off-resonant spectrum in Fig. 3a, appears in the on-resonant one in Fig. 3b, distinctly. The T_K of $CePd_3$ has been reported to be about 240 K and that of $CeSn_3$ to be about 200 K [20,21]. They have very similar Kondo temperature. It is interesting that the relative f^1 peak of $CeSn_3$ is much smaller than that of $CePd_3$ irrespective of similar T_K. This directly indicates the fact that there is a big difference in the initial state configurations, i.e. in the 4f occupancy n_f, between $CePd_3$ and $CeSn_3$ [10].

The f^2 spectrum in Fig. 3b exhibits a single peak without the shoulders observed in off-resonant spectra in Fig. 3a. The f^2 peaks of $CeRh_3$ and $CeSn_3$ are located at about 4.8 and 4.0 eV, respectively. The difference in the f^2 peak line-shape between the off- and the on-resonant spectra is caused by the partly enhanced multiplet structure by the resonance effects. Fig. 4 shows E_{ex} dependence of the RIPE spectra of $CeRh_3$. The multiplet structures are indicated by the vertical bars and dashed lines. A dramatic change in spectral lineshape of the f^2 peak is observed as the E_{ex} changes. This is caused by the transfer of spectral weights between the multiplet structures at the f^2 final states. In order to interpret this E_{ex} dependence of the f^2 peak, we have to take

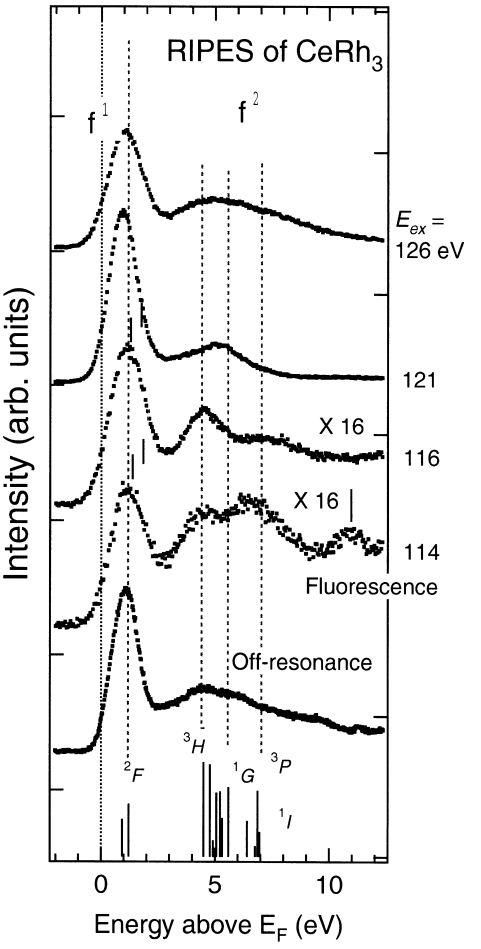

Fig. 4. The RIPE spectra of $CeRh_3$ at several excitation energies. The numbers written on the side of the right axis represent E_{ex}. The calculated multiplets in $4f^1$ and $4f^2\underline{c}$ final state configurations are added at the bottom axis. The structure indicated by vertical bar in the spectrum at $E_{ex}=114$ eV is the normal fluorescence.

the selection rule in the final state on resonance into account [8,9].

In Fig. 4 all the $4f^2$-multiplet components are convoluted with the experimental resolution in the off-resonant spectra and cannot be clearly distinguished. In the spectrum at $E_{ex}=114$ eV, which is situated just below the giant-resonance, the f^2 peak is clearly split into two peaks. These two peaks are also reproduced in the IAM calculation [10] and are roughly assigned to ^3H and ^3P components. The spectral weight of the ^3P component is weakened as E_{ex} increases from 116 to 126 eV in Fig. 4. The multiplets at higher energy side ($^1D\sim{}^1I$) are not enhanced at this lower E_{ex} range of the resonance (see Fig. 5). On the other hand, the multiplets around 5 eV ($^3H\sim{}^1G$) are resonantly enhanced in this range of E_{ex}. To interpret the E_{ex} dependence of the resonance effects on the muliplet components, the following intuitive discussion, based on the very simple model, is presented [8,9]. The proper analysis by using the IAM calculation was presented in Refs. [8–10]. In the off-resonant region the selection rule of RIPE process is not strict, i.e. the electrons added to the 4f level can have either up or down-spin configurations. Therefore, all multiplet components corresponding to possible final states can be observed. On the resonance, the intermediate state with the created 4d-hole spin occurs with the large multiplet splitting of $|\underline{4d}\ 4f^3\rangle$ state concerning the arrangement of two 4f electrons and 4d-hole spin. The intermediate state with three up-spin 4f electrons and an up-spin 4d hole gives the lowest energy under the restriction of the dipole selection rule. This intermediate state decays into the triplet final state at the resonance. In contrast, the highest energy intermediate state with two down-spins and one up-spin 4f electrons and a down-spin 4d hole makes transition into the singlet final state. Therefore, the spectrum of the triplet state at the lower energy side is enhanced by lower E_{ex} and the one of the singlet state at the higher energy side is enhanced at higher E_{ex}. Accordingly, the spectral intensity of the f^2 peak shifts from lower to higher energy side as E_{ex} increases in the giant resonance.

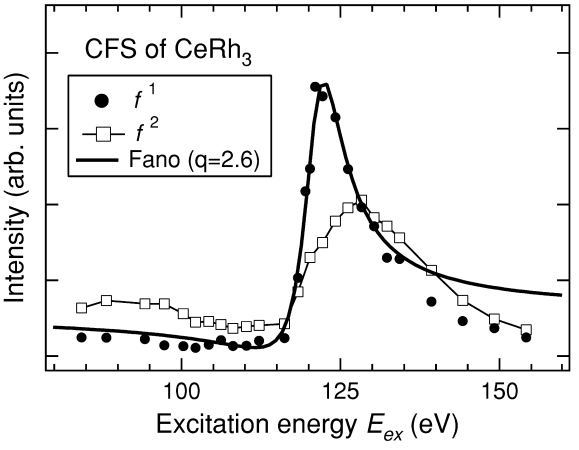

Fig. 5. The CFS curves for the $4f^1$ and $4f^2$ final states. The spectrum was obtained by plotting the integrated intensities of f^1 and f^2 peaks against the excitation energy E_{ex}.

The constant final state (CFS) spectra of RIPE in $CeRh_3$ are shown in Fig. 5. The spectra are obtained by plotting the integrated intensities of the f^1 and the f^2 peaks against E_{ex} [3–7]. Around 120 eV of E_{ex}, the giant-resonance takes place, which causes great enhancements of the f^n curves. Resonant effect can lead to very dramatic variations in IPE-matrix element for very small changes in E_{ex} at the threshold. The f^1 and the f^2 curves reach a maximum at about 121 and 127 eV, respectively, and slowly decrease as the E_{ex} increases. The asymmetric line-shapes of both curves represent a very large multiplet splitting of the intermediate state and the existence of the Fano-type interference, although the CFS at the M_5 edge have symmetric lineshapes [3–7]. This difference in CFS, that is to say the difference in the resonance effects between the M_5 and the $N_{4,5}$ edge is reminiscent of the XAS case. The asymmetric $N_{4,5}$-CFS indicates strong interactions between the 4d and the 4f states due to a larger overlap of wave functions.

4.2. Resonance effects at the $N_{4,5}$ pre-threshold region

The giant-absorption bands in the XAS have very wide and asymmetric lineshapes due to the autoionization effect in contrast with the 3d-absorption. On the other hand, the final states at the pre-threshold XAS are prevented by the centrifugal barrier of the 4d-core hole and have longer life-time and thus give sharp peaks. Therefore, we expect weak but clear resonance-enhancements of RIPE spectra at the pre-

threshold. The 'excitonic' final states of the pre-threshold absorption occurs also through the Coulomb scattering between the 4d-core and incoming electrons and some of them can become the intermediate states of the RIPE process which radiatively decay into the RIPE final states. In addition, at the pre-threshold the resonance effects of the RIPE spectra are expected to be much clearer because of autoionization effect and normal fluorescence affects the spectrum less.

Fig. 6a shows RIPE spectra of $CePd_3$ measured below the $N_{4,5}$ edge [26]. The excitation energies, E_{ex} are given at the left side of the spectra. Marked excitation energy dependence of the f peaks are clearly observed in Fig. 6a. It is pointed out that the pre-threshold resonance is dissimilar to the giant-resonance [10]. The resonance-enhancement of the f peaks at the pre-threshold springs up in a narrower range of E_{ex} and occurs twice at E_{ex} ~105 and about 110 eV. In Fig. 7 the CFS of the f^1 peak are shown, which are measured below and above the threshold [3–7]. The CFS explicitly show the difference in the resonance behavior between the pre-threshold- and giant-resonance. The CFS of the giant-resonance, which has an asymmetric broad lineshape, is reminiscent of the giant-absorption band in the 4d-XAS [19]. On the other hand, the pre-threshold CFS has a sharp form which is similar to the XAS below the threshold. The sharpness of the pre-threshold-resonance is due to the relatively stable intermediate states, that is to say its longer life time, in contrast to the giant-resonance.

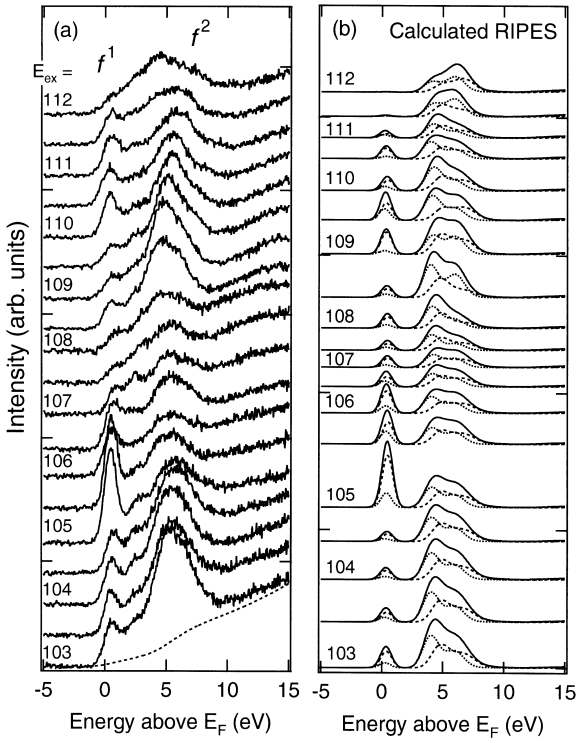

Fig. 6. (a) The experimental RIPE spectra and (b) the calculated RIPE spectra at the $N_{4,5}$ pre-threshold of $CePd_3$. The numbers beside the left axes stand for the excitation energy E_{ex}. The broken and the dotted-lines stand for the bulk and the surface spectra, respectively. The calculated spectra are broadened with a Gaussian function of width 0.5 eV (HWHM) in order to include the overall resolution and a Lorentzian function with the energy dependent life-time width $\Gamma = 0.5 + 0.01|E - E_F|^2$ eV.

The f^n peak's lineshapes widely vary with E_{ex} in Fig. 6a. It seems to be natural to attribute the changes of the f^2 peak lineshapes to the multiplet splitting of the $|4f^2\underline{c}\rangle$ final states as discussed above. Each of the multiplets is resonantly excited at different E_{ex}. Accordingly, the f^2 peak-resonance has a strong dependence on E_{ex}. On the other hand, the f^1 peak is found to be intensely enhanced around $E_{ex} = 105$ eV and a weaker enhancement is observed at higher E_{ex} ~110 eV. The calculated RIPE spectra at the $N_{4,5}$ pre-threshold are shown in Fig. 6b [26]. Superposing these bulk and surface spectra with a ratio of 1:1 makes up a total spectrum (full line). The parameter set for the calculation is listed in Table 1. We derived the bulk and surface parameters from the

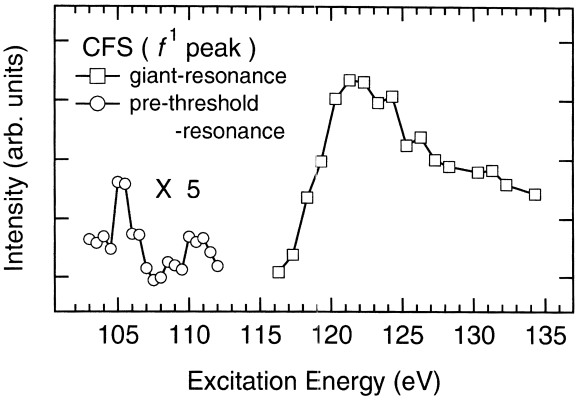

Fig. 7. CFS of the giant- and pre-threshold-resonance. The spectra are obtained by plotting the integrated intensities of the f^1 peaks against the E_{ex}.

Table 1
The parameter sets for $CePd_3$ and the calculated average 4f-number n_f. U_{ff} (=6.4 eV) and U_{fc} (=9.5 eV) are the same values for both the bulk and surface

	ε_f (eV)	V (eV)	n_f
Bulk	−1.8	0.36	0.92
Surface	−2.3	0.28	1.0

analysis of the spectra (3d-XPS, X-BIS, M_5-RIPE and $N_{4,5}$-RIPE spectra) which possess various bulk-sensitivity. ε_f, U_{ff} and V are the 4f level, Coulomb potential between the 4f electron and the hybridization strength between the 4f and conduction states, respectively. U_{fc} represents the attractive potential between the 4f electron and 4d core-hole. It is shown that the calculated RIPE spectra reproduce the observed ones in Fig. 6a at almost the whole pre-threshold region, especially the strong enhancement of the f^1 peak in RIPE spectra at 105 eV as well as the complicated resonant behavior of ^3H and ^1G multiplets in the f^2 peak.

In order to investigate the multiplet structure in the intermediate states of the RIPE process, the calculated resonant-excitation probability to the intermediate states, P(E_{ex}) are shown in Fig. 8. Fig. 8a shows the calculated total − P(E_{ex}). The P(E_{ex}) stands for the absorption intensities by inverse super Coster–Kronig transition, $|4f^n\underline{c}\varepsilon l\rangle \rightarrow |\underline{4d}\ 4f^{n+2}\underline{c}\rangle$, ($n=0$, 1) [26]. Here the εl is the incoming electron with angular momentum l and energy E_{ex}. Those transitions are equal to the excitation processes into the intermediate states of the RIPE processes of the f^1 and the f^2 peaks. Therefore, P(E_{ex}) intensity approximately accounts for a resonance-enhancement of the RIPE spectrum. It is found that the strong absorption intensity at $E_{ex}=105$ eV in the P(E_{ex}) is mainly concerned with the $|\underline{4d}\ 4f^2\rangle$ final state in ^4G multiplet. From a straightforward comparison with the RIPE spectra in Fig. 6a, the intense peak of ^4G explains the dramatic enhancement of the f^1 peak in the RIPE spectra around $E_{ex}=105$ eV. In addition, the weaker resonance of the f^1 peak around 110 eV corresponds to the structures located between 108 and 111 eV in the P(E_{ex}). It should be noted that the resonance process is a second-order optical process, which is caused by the excitation to the intermediate state. The ^4G final state of the P(E_{ex}), which is

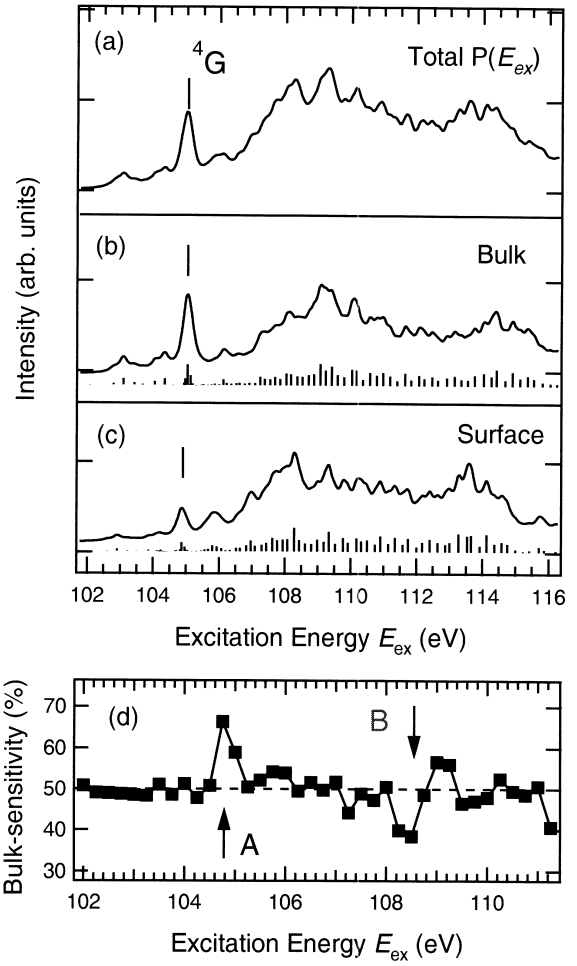

Fig. 8. The calculated P(E_{ex}) at the pre-threshold region of $CePd_3$. (a) Total spectrum, which is obtained by superposing the bulk and the surface spectra with the ratio of 1:1. (b) and (c) is bulk and surface spectrum, respectively. (d) The calculated bulk-sensitivity I(Bulk)/I(Total) as a function of E_{ex} where I(Bulk) and I(Total) stand for the integrated-intensities of the bulk- and bulk + surface spectra. The calculated spectra are broadened with a Lorentzian function of width 0.15 eV (HWHM).

excited by the scattering between the εg ($l=4$) and 4d-core electrons, radiatively decays into the ^2F final states of the RIPE process. The $^4G \rightarrow {}^2F$ transition becomes weakly dipole-allowed due to an admixture of ^2G states through a spin–orbit interaction. In the giant-resonance region, ^2S, ^2D, ^2G, ^2I and ^2L intermediate states are excited through the 4d εl–4f 4f Coulomb scattering. With a restriction by the dipole selection-rule, ^2D and ^2G intermediate states give rise

to dramatic resonance-enhancements of the f^1 peak. These states mix with the quartet states, ^4P, ^4D, ^4F, ^4G, ^4H and ^4I, so they have weak weights in the pre-threshold region.

5. Surface electronic states measured by RIPE spectroscopy

RIPE measurement is a surface-sensitive technique as well as other high-energy spectroscopies. Especially, the RIPE spectrum at the $N_{4,5}$ edge has a great deal of surface contribution due to the short penetration depth of the incident electron. It is troublesome to pick up the bulk contribution from the spectra without the help of calculation because it strongly mixes with the surface contribution.

We present, here, the surface effects on the pre-threshold RIPE spectra as one example. Detailed discussion about the surface effects on the giant-resonance spectra was presented in Refs. [25,26].

We show the interesting connection between the above resonance effects on the f^1 peak and bulk-sensitivity of the pre-threshold RIPE spectrum. The calculated $P(E_{ex})$ for the bulk and the surface are shown in the Fig. 8b and c, respectively. It should be noted that the sharp peak ^4G in the bulk spectrum is much larger than that in the surface spectrum. Because of the localized feature of the surface 4f electron, as shown in Table 1, the weight of the $4f^0$ configuration in the initial state of the surface is very small. Accordingly, the probability of the $|\underline{4d}\ 4f^2\rangle$ final state (this is corresponding to the intermediate state for the RIPE) is strongly suppressed in the surface $P(E_{ex})$ as compared with the bulk spectrum. As a result, the ^4G ($\underline{4d}$, $4f^2$) peak is weakened in the surface spectrum. On the other hand, there is large intensity of $\underline{4d}\ 4f^3\ \underline{c}$ multiplets distributed over the relatively higher energy region above 107 eV. Therefore, there is a strong admixture between the bulk and surface contribution to the RIPE spectra above $E_{ex}=107$ eV. This resonance feature is characteristic of the pre-threshold region. In the giant-resonance, the $\underline{4d}\ 4f^2$ and $\underline{4d}\ 4f^3\ \underline{c}$ multiplet structures in the intermediate state strongly mix with each other due to their very short lifetime over the whole energy region. Therefore if E_{ex} is tuned to the sharp ^4G peak we can obtain the spectrum which includes a relatively larger bulk contribution. When ^4G is resonantly excited a large resonance-enhancement of the f^1 peak with a dominant bulk contribution occurs. Simultaneously, the resonance-enhancement of the bulk f^2 peak also occurs through the hybridization effects in the intermediate and final states. Fig. 8d shows the calculated bulk-sensitivity in the lower side of the pre-threshold region. The bulk-sensitivity was obtained from the calculated RIPE spectra in Fig. 8b (see the caption). We can find, in fact, a sharp peak around 104.75 eV (A) and, unexpectedly, a dip around 108.5 eV (B). The former realizes the high bulk-sensitivity around $E_{ex}=105$ eV as discussed above. Moreover, the latter indicates the existence of a 'surface-sensitive' excitation energy range as in the case of the bulk. We can effectively probe the unoccupied bulk or surface 4f electronic states by the measurements at E_{ex} ~104.75 and 108.5 eV, respectively.

In Fig. 9 the RIPE spectra are measured at E_{ex} ~104.7, 108.5 and 121.5 eV. $E_{ex}=121.5$ eV causes the greatest enhancement of the f^1 peak in the giant-resonance as shown in Fig. 7. As mentioned above, the spectrum at 121.5 eV also contains considerable surface contribution. The f^2 peaks in the spectra at 108.5 and 121.5 eV are situated at the lower energy side as compared with the one at 104.7 eV. The f^2 peak position in the spectrum at 104.7 eV is rather similar to that of the X-BIS spectrum which is measured at 1486.6 eV [27]. X-BIS is a relatively bulk-sensitive technique due to a somewhat longer probing depth. This is evidence of the higher bulk-sensitivity of the spectrum measured around 105 eV. It should be noted that the larger intensity of the f^1 peak at 104.7 eV is caused by the resonance effect and the spectra does not give an exact replica of the unoccupied DOS of $CePd_3$. We can derive the intrinsic information about the energy positions of the bulk f^1 and the f^2 peaks from the spectra. On the other hand, the surface-sensitive spectrum measured at 108.5 eV has a very small f^1 peak and the f^2 peak is shifted to the lower energy side by 0.8 eV as compared to the spectra at 104.7 eV. This 'surface-shift' in f^2 peak is mainly caused by the difference in ε_f as shown in Table 1. This result shows the localized character of the surface 4f electron and is consistent with the fact that many mixed-valent systems have a γ-like electronic structure in the

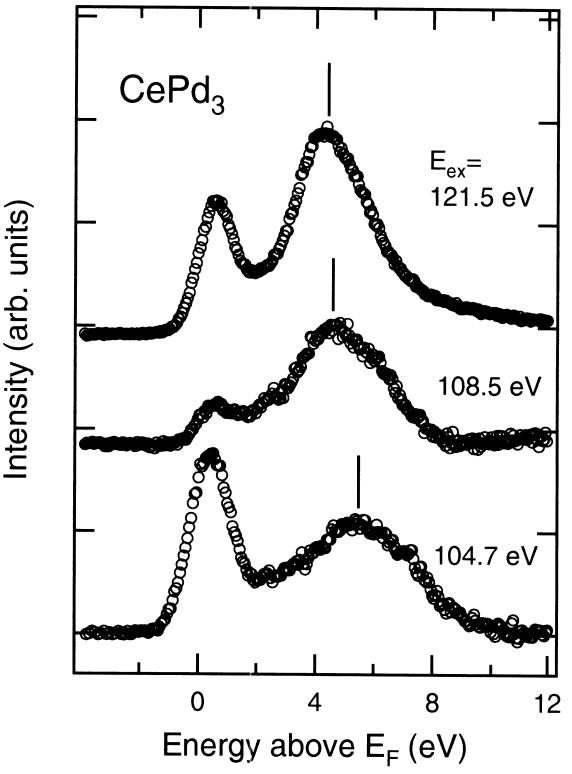

Fig. 9. The experimental RIPE spectra of $CePd_3$ which are measured at 104.7, 108.5 and 121.5 eV. The background is subtracted from the spectra. The vertical bars represent the energy position of the f^2 peaks.

surface region whereas they present a strongly α-like behavior in the bulk [28,29].

This unique bulk- (or surface-) sensitivity is based on the following properties of the pre-threshold-resonance; (1) the difference in the intermediate state energy of the bulk- and surface-resonance processes. This is caused by the difference in the parameters and the 4f occupation. (2) The narrower lifetime-width of the multiplets which have excitonic feature at the pre-threshold. As a result of (1) and (2), we can selectively excite the specific intermediate state (e.g. ^4G). Application of this phenomenon to the other materials will yield a powerful tool for investigating the bulk and the surface unoccupied electronic structure. However, the problem whether this unique relationship between the bulk- (or surface-) sensitivity and the resonance effects at the pre-threshold holds in other materials still remains open.

6. Temperature dependence of RIPE spectra

Malterre et al. reported the temperature dependence of the BIS of $CePd_3$ and $CeSi_2$ [30]. The destruction of the Kondo effect at $T > T_K$ is strongly reflected in the RIPE (or BIS) spectra. Roughly speaking, the reason for this high sensitivity of RIPE spectra to the 4f electronic state is that Kondo resonance exists just above E_F. In this section, we present the temperature dependence of RIPE spectra of the pseudoternary compounds $CeCoGe_{3-x}Si_x$ to show the systematic T_K dependence of the temperature-dependent RIPE spectra.

The nature of $CeCoGe_{3-x}Si_x$ series of compounds has been investigated by measuring magnetic susceptibility, electronic resistivity and specific heat [31,32]. Substitution of silicon for germanium produces the normal chemical pressure effect and which reduces the unit-cell volume by about 10% from $CeCoGe_3$ to $CeCoSi_3$. The antiferro coupling constant J is thereby enhanced as the silicon concentration x increases and the antiferromagnetism in $CeCoGe_3$ is suppressed around $x = 1.2$ by the enhanced Kondo effect. The overall behavior of this system is qualitatively understood within Doniach's magnetic phase diagram [31,32]. $CeCoGe_{3-x}Si_x$ is therefore a unique test case for which T_K can be considerably varied by simply changing the composition x in a single system [31,32].

Fig. 10 shows RIPE spectra of $CeCoGe_{3-x}Si_x$ ($x = 0$, 1.0, 1.5, 2.0, 3.0) measured at the $N_{4,5}$ edge [33]. The results in Fig. 10 show the changes in the unoccupied 4f-state with continuous rise of the J as x increases. The clear reduction of the f^1 peak is observed as x decreases. The intensity of the f^1 peak of $CeCoSi_3$ is reduced by ~35% as compared with the $CeCoGe_3$ one. The reduction from $x = 3.0$ to 1.5 is most remarkable. The decrease in T_K causes the dramatic transformation of the Kondo resonance.

The RIPE spectra of $CeCoSi_3$ are displayed as a function of temperature up to 285 K in Fig. 11. Continuous and striking reduction of the f^1 peak has been measured as temperature rises. We define the ratio r_f of the f peaks by the following equation as a direct indicator of the n_f

$$r_f = I[f^2]/(I[f^1] + I[f^2]).$$

Here, $I[f^n]$ represents the integrated intensities of

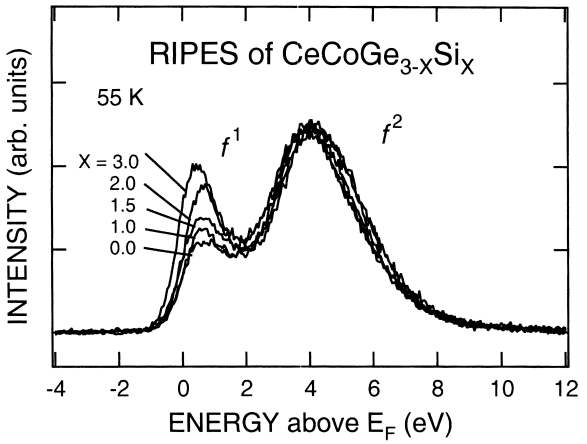

Fig. 10. The RIPE spectra of $CeCoGe_{3\ to\ x}Si_x$ $(0<x<3)$ measured at 55 K. The integrated backgrounds were subtracted from the spectra. The spectral intensities are normalized by f^2 peak intensities.

the f^n peak. We can estimate the reliable value $I[f^n]$ by the dramatic resonance-enhancements of the f peaks. The r_f does not give the exact n_f, but the r_f still directly reflects the n_f well and is a very useful quantity in the following discussion. The r_fs of several compounds of $CeCoGe_{3-x}Si_x$ are plotted against temperature in Fig. 12. The r_fs except for $x=3.0$ slightly rise with temperature up to 285 K. The relatively constant r_fs of $x=1.0$ and 0.0 reflect

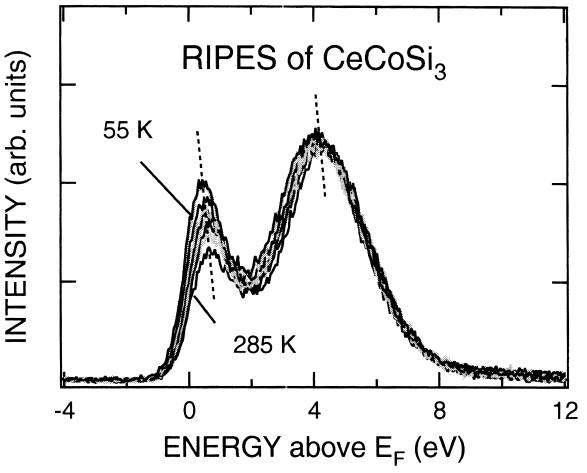

Fig. 11. The RIPE spectra of $CeCoSi_3$ as a function of the temperature. The spectral intensities are normalized by f^2 peak intensities.

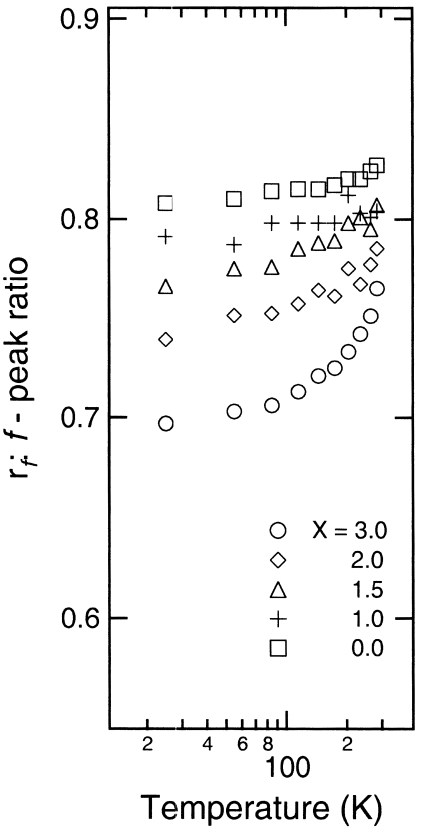

Fig. 12. The f-peak ratio: r_f as a function of x which is plotted against temperature T.

the stable 4f electron numbers $n_f \sim 1$, that is, the paramagnetic state with an effective magnetic moment close to the value of Ce^{3+}. On the other hand, r_f of $x=3.0$, for which the extremely high T_K (of the order of 900 K) has been reported [31,32], shows a dramatic rise from about 200 to 285 K. This rise directly indicates the destruction of the Kondo effect on each Ce site and n_f increases as temperature rises. As shown by Bickers et al., the transport and thermodynamic properties of mixed valence Ce systems are represented by universal functions scaled by T_K in the impurity systems [34]. And the scaling behaviors in the high energy spectroscopic results of the several Ce compounds have been explained within the impurity model [30,35] and the Kondo effect which dominates the Ce-based heavy fermion systems is generally accepted to be well understood in the dilute limit. The results in Fig. 12 give

evidence of the Kondo-scaling behavior in the $CeCoGe_{3-x}Si_x$ systems. It should be noted, however, that the onset of the rise of the r_f sets in at a sufficiently lower temperature (~200 K) than the single-impurity T_K which is estimated from the specific heat coefficient within the framework of the Coqlin–Shriefer model [36]. This fact indicates the existence of the smaller energy scale $k_B T^*$ of the system. The T^* value appears to correspond to the temperature where the maximum value of magnetic susceptibility is found ($T_\chi^{max} = 230$ K) [31,32]. The paramagnetic state with local moments is sustained far below T_K. It should be noted that the T^* of $CeCoGe_{3-x}Si_x$ is much smaller than the single-impurity T_K. A similar scaling behavior by T^* was reported in the $CeRu_2(Ge_{1-x}Si_x)_2$, although its T^* is comparable to the T_K [37]. This strong material dependence of T^* suggests that the relationship between T^* and T_K is not fixed and straightforward even in the spin fluctuation systems with large J.

7. Summary

We present the results of the RIPE spectra at the Ce $N_{4,5}$ absorption edge of several intermetallic Ce compounds. The clear resonance effects are observed although a weaker degree of the resonance-enhancements than that at the M_5 edge [3–7]. The calculation within the IAM framework, which includes the full-multiplet coupling effects, explain well the RIPE spectra at almost the whole $N_{4,5}$ absorption region. Weak but sharp pre-threshold RIPE spectra are observed. Considerably different resonance behaviors between the bulk- and the surface-4f regions are observed at the $N_{4,5}$ pre-threshold of $CePd_3$. The T_K dependence of the temperature-dependent RIPE spectra are clearly observed in $CeCoGe_{3-x}Si_x$ compounds. Especially in the systems with high T_K, the dramatic temperature dependence of the RIPE spectra are observed. This result shows that the collective dense Kondo state at low temperature is already destroyed at $T \ll T_K$.

At present, the RIPE spectroscopy developed into the most powerful tool for the study of the SCE systems. However, now, the energy resolution of the RIPE measurement is much poorer than that of the PE measurement. The improvement in the energy resolution, especially in the monochromatization of the electron-flux, is desired.

Acknowledgements

We would like to express to our collaborators deepest gratitude. We thank Prof. A. Kotani, Prof. J.C. Parlebas and Dr. T. Uozumi for their meaningful discussion. We are thankful to Dr. G. Schmerber and Dr. J.P. Kappler for preparations of $CePd_3$, $CeSn_3$ and $CeSn_3$ samples. We are thankful to Dr. D.H. Eom and Prof. M. Ishikawa for preparations of $CeCoGe_{3-x}Si_x$ compounds.

References

[1] R.J. Liefield, A.F. Burr, M.B. Chamberlain, Phys. Rev. A 9 (1974) 316.
[2] M.B. Chamberlin, A.F. Burr, R.J. Liefield, Phys. Rev. A 9 (1974) 663.
[3] P. Weibel, M. Grioni, D. Malterre, B. Dardel, Y. Baer, Phys. Rev. Lett. 72 (1994) 1252.
[4] M. Grioni, P. Weibel, D. Malterre, F. Jeanneret, Y. Baer, G. Olcese, Physica B. 206–207 (1995) 71.
[5] M. Grioni, P. Weibel, D. Malterre, Y. Baer, D. Duo, Phys. Rev. B 55 (1997) 2056.
[6] P. Weibel, M. Grioni, C. Heche, Y. Baer, Rev. Sci. Instrum. 66 (1995) 3755.
[7] P. Weibel, M. Grioni, D. Malterre, O. Manzardo, Y. Baer, G.L. Olcese, Europhys. Lett. 29 (1995) 629.
[8] A. Tanaka, T. Jo, Physica B. 206–207 (1995) 74.
[9] A. Tanaka, T. Jo, J. Phys. Soc. Jpn. 65 (1996) 615.
[10] K. Kanai, Y. Tezuka, T. Terashima, Y. Muro, M. Ishikawa, T. Uozumi, A. Kotani, G. Schmerber, J.P. Kappler, J.C. Parlebas, S. Shin, Phys. Rev. B 60 (1999) 5244.
[11] S. Hüfner, in: Photoelectron Spectroscopy, Springer Series in Solid-State Sciences, 1995, p. 90.
[12] H. Ishii, K. Kanai, Y. Tezuka, S. Shin, J. Electron Spectrosc. Relat. Phenom. 92 (1998) 77.
[13] U. Fano, Phys. Rev. 124 (1961) 1866.
[14] K. Kanai, Doctor thesis, University of Tokyo, 2000.
[15] Y. Tezuka, private communication.
[16] A. Tanaka, T. Jo, J. Phys. Soc. Jpn. 66 (1997) 1591.
[17] C. Guillot, Y. Ballu, J. Paigne, J. Lecante, K.P. Jain, P. Thiry, R. Pinchaux, Y. Petroff, L.M. Falicov, Phys. Rev. Lett. 39 (1977) 1632.
[18] S. Shin, A. Agui, M. Fujisawa, Y. Tezuka, T. Ishii, N. Hirai, Rev. Sci. Instrum. 66 (1995) 1584.
[19] G. Kalkowski, C. Laubschat, W.D. Brewer, E.V. Sampathkumaran, M. Domke, G. Kaindl, Phys. Rev. B 32 (1985) 2717.

[20] M.J. Besnus, J.P. Kappler et al., J. Phys. F 13 (1983) 157.
[21] J.G. Sereni, J. Less-Common Metals 84 (1982) 1.
[22] J.G. Sereni, O. Trovarelli, A. Herr, J.Ph. Schillé, E. Beaurepaire, J.P. Kappler, J. Phys.: Condens. Matter 5 (1993) 2927.
[23] J.P. Kappler, P. Lehman, G. Shmerber, G.L. Nieva, J.G. Sereni, J. Phys. (Paris) 49 (1988) C8–721.
[24] J.P. Kappler, G. Shmerber, J.G. Sereni, J. Magn. Magn. Mater. 79–77 (1988) 185.
[25] K. Kanai, Y. Tezuka, M. Fujisawa, Y. Harada, S. Shin, G. Schmerber, J.P. Kappler, J.C. Parlebas, A. Kotani, Phys. Rev. B 55 (1997) 2623.
[26] K. Kanai, T. Terashima, A. Kotani, T. Uozumi, G. Schmerber, J.P. Kappler, J.C. Parlebas, S. Shin, Phys. Rev. B 63 (2001) 33106.
[27] Y. Baer, H.R. Ott, J.C. Fuggle, L.E. De Long, Phys. Rev. Lett. 24 (1981) 5382.
[28] C. Laubshat, E. Weschke, C. Holtz, M. Domke, O. Strebel, G. Kaindl, Phys. Rev. Lett. 65 (1990) 1639.
[29] G. Krill, J.P. Kappler, A. Meyer, L. Abadli, M.F. Ravert, J. Phys. F 11 (1981) 1713.
[30] D. Malterre, M. Grioni, P. Weibel, Y. Baer, Phys. Rev. Lett. 68 (1992) 2656.
[31] M. Ishikawa, D.H. Eom, N. Takeda, K. Kanai, M. Watanabe, S. Shin, Jpn. J. Appl. Phys. Ser. 11 (1999) 171.
[32] D.H. Eom, M. Ishikawa, J. Kitagawa, N. Takeda, J. Phys. Soc. Jpn. 67 (1998) 2495.
[33] K. Kanai, T. Terashima, D.H. Eom, M. Ishikawa, S. Shin, Phys. Rev. B 60 (1999) R9900.
[34] N.E. Bickers, D.L. Cox, J.W. Wilkins, Phys. Rev. B. 36 (1987) 2036.
[35] K. Kanai, Y. Tezuka, H. Ishii, S. Nozawa, S. Shin, A. Kotani, G. Schmerber, J.P. Kappler, J.C. Parlebas, J. Electron Spectrosc. Relat. Phenom. 92 (1998) 81.
[36] B. Coqblin, J.R. Schrieffer, Phys. Rev. 185 (1969) 847.
[37] S. Süllow, M.C. Aronson, B.D. Rainford, P. Haen, Phys. Rev. Lett. 82 (1999) 2963.